

# Normal fluid eddies in the thermal counterflow past a cylinder

Y. A. Sergeev<sup>1</sup> and C. F. Barenghi<sup>2</sup>

<sup>1</sup>*School of Mechanical and Systems Engineering, Newcastle University,  
Newcastle upon Tyne NE1 7RU, United Kingdom*

<sup>2</sup>*School of Mathematics and Statistics, Newcastle University,  
Newcastle upon Tyne NE1 7RU, United Kingdom*

(Dated: November 16, 2018)

## Abstract

A recent Particle Image Velocimetry (PIV) experiment in He II counterflow around a cylindrical obstacle showed the existence of apparently stationary normal fluid eddies both downstream (at the rear) and upstream (in front) of the cylinder. This rather surprising result does not have an analogue in experimental observations of classical fluid flows. We suggest that the explanation for the apparent stability of such eddies can be provided entirely from the viewpoint of classical fluid dynamics. We also discuss a possible connection between the emergence of the normal fluid eddies and the polarization of the vortex tangle in superfluid.

PACS numbers: 67.40.Vs, 47.37.+q, 47.27.-i

## I. MOTIVATION

Particle Image Velocimetry (PIV), which has been, for several decades, a standard technique of flow visualization in classical fluid dynamics, is based on tracking the motion of solid particles injected into the fluid. Provided the particles are sufficiently small, they can be expected to follow faithfully the fluid flow.

Recently implemented in helium II [1], the PIV technique has already yielded some non-trivial and unexpected results [2, 3, 4, 5] followed by the attempts of their theoretical interpretation (see e.g. Refs. [6, 7]). Among surprising experimental results is the recent observation [3] of the apparently stationary normal fluid eddies in the thermal counterflow past a cylinder. In the cited work, Zhang and Van Sciver visualized the motion of small particles in the thermal counterflow around the cylinder of diameter  $D = 0.635$  cm fixed in the center of rectangular channel of a cross-section  $3.89 \times 1.95$  cm<sup>2</sup>. The counterflow was produced, in two separate experiments, by the heat flux  $q = 0.4$  and  $1.12$  W/cm<sup>2</sup> at temperatures  $T = 1.6$  and  $2.03$  K, respectively (corresponding to the Reynolds numbers  $\text{Re}_D = \rho D v_n / \mu_n = 4.1 \times 10^4$  and  $2.1 \times 10^4$ , where  $\rho = 0.145$  g/cm<sup>3</sup> is the density of the liquid helium, and  $v_n$  and  $\mu_n$  are the mean velocity and the viscosity of the normal fluid). Solid particles used for visualization in the PIV experiments were polymer microspheres of diameter  $1.7$   $\mu\text{m}$  and density  $1.1$  g/cm<sup>3</sup>.

In these experiments Zhang and Van Sciver observed the formation of large-scale eddies of the particulate motion located both downstream and, surprisingly, upstream of the cylinder with respect to the normal flow (it should be noted that these structures were somewhat more discernible in the second of two experiments, i.e for  $\text{Re}_D = 2.1 \times 10^4$ , in which case the corresponding mean normal fluid velocity was  $v_n \approx 2.2$  cm/s). These, apparently stable vortices of the particulate flow field were located at distances about 3 cylinder radii from its center at the angles  $\pm 45^\circ$  and  $\pm 135^\circ$  to the axis along the undisturbed flow through the center of the cylinder.

In order to interpret these observations, the following question should first be addressed: what do tracer particles actually trace? It seems natural to assume that in the cited experiment, because the Stokes drag of small particles is much larger than other forces exerted by the normal fluid (see e.g. Ref. [6]), the particle trace the normal fluid. However, solid particles also interact strongly with quantized vortices which may reconnect to the particle

surface; such interactions may lead to the appearance of the additional force exerted on particles by the superfluid. This additional force was actually measured in another Zhang and Van Sciver's experiment [2] on particle sedimentation in the thermal counterflow, and later analyzed theoretically [7] by the authors of the present work.

A second question is: do the circulation cells of the particulate motion map, in the experiment [3], the normal eddies, or result from complex interactions of particles with both the normal fluid and quantized vortices in the superfluid component (in which case the eddies in the normal fluid may not even exist)? Since in this experiments the vortex tangle was relatively dilute (see more detailed discussion below in Sec. V), we can expect with some confidence that the particle motion indeed maps, at least qualitatively, the normal flow. The observed normal flow patterns do not have a classical analogue: in classical fluid dynamics, stationary eddies upstream of the cylinder have never been observed, and downstream of the cylinder one would rather expect the Von Kármán vortex street than a pair of apparently stationary eddies. In Ref. [3] it was suggested that the observed large normal vortex structures were caused by the complex interaction between the two fluid components of He II.

In the present work we argue that, while the emergence of the large-scale vortex structures is, most likely, caused by the mutual friction between quantized vortices and the normal fluid, the apparent stability of the observed eddies, both at the rear and in front of the cylinder, can be explained entirely from the viewpoint of classical fluid dynamics without invoking an interaction between the normal fluid and superfluid vortices.

Because the Reynolds numbers in the cited experiment were large ( $\sim 10^4$ ), instead of considering the turbulent viscous flow past a cylinder we will analyze a much simpler model of the plane motion of two point vortices of opposite polarities in the inviscid, potential flow around a disk. We shall show that there exist stationary configurations of the vortex-antivortex pair, both behind and in front of the disk. Such configurations are unstable, i.e. any perturbation of the stationary configuration leads to eventual sweeping of the vortex points away from the disk. However, we shall show that there exist stationary configurations such that, on the time scale corresponding to the duration of experiment [3], the vortices located sufficiently close to the corresponding stationary points will remain in the close proximity of their initial locations. Moreover, such stationary points are positioned as the apparently stable eddies seen by Zhang and Van Sciver. In conclusion we shall also discuss

a possible connection between the emergence of the normal fluid eddies and the polarization of the vortex tangle in the superfluid component of He II.

## II. LAGRANGIAN EQUATIONS OF MOTION OF POINT VORTICES IN THE INVISCID FLOW AROUND THE DISK

We consider the two-dimensional inviscid, potential flow, with velocity  $U$  at infinity, around a circular disk of radius  $a$ . We are concerned with a motion in such a flow of a vortex-antivortex pair, i.e. of two vortices of opposite polarities but the same circulation,  $\Gamma$ . Let the positions of the vortex points on the complex plane be  $z_1(t) = x_1(t) + iy_1(t)$  and  $z_2(t) = x_2(t) + iy_2(t)$ , see Fig. 1. The reason why the vortex  $z_1$  has negative (clockwise) circulation,  $\Gamma < 0$ , will become clear in Sec. III.

Each of these vortices moves as a fluid point in the superposition of the imposed flow around the disk and the flow field of another vortex. Complex potential of the superposition of the potential, uniform at infinity, flow around the disk and the flow created by the vortex point at, say,  $z = z_1$  is [8]

$$w(z) = U \left( z + \frac{a^2}{z} \right) + \frac{\Gamma}{2\pi i} \left[ \ln(z - z_1) - \ln \left( \frac{a^2 - zz_1^*}{z} \right) \right], \quad (1)$$

where  $z^* = x - iy$  denotes the complex conjugate of  $z = x + iy$ .

It is convenient to introduce the non dimensional variables

$$z' = \frac{z}{a}, \quad w' = \frac{w}{Ua}, \quad \lambda = -\frac{\Gamma}{4\pi Ua} > 0, \quad (2)$$

so that the non-dimensional complex potential is (from now on the primes are omitted)

$$w(z) = z + \frac{1}{z} + 2i\lambda \ln \frac{z(z - z_1)}{1 - zz_1^*}. \quad (3)$$

The  $x$ - and  $y$ -components of the fluid velocity are, respectively,  $u = \text{Re} \{dw/dz\}$  and  $v = -\text{Im} \{dw/dz\}$ .

The flow potential (3) yields the following Lagrangian equations of motion of two vortex points,  $z_1(t)$  and  $z_2(t)$ :

$$\frac{dx_j}{dt} = \text{Re} \{f_j(z_1, z_2)\}, \quad \frac{dy_j}{dt} = \text{Im} \{f_j(z_1, z_2)\}, \quad (4)$$

where  $j = 1, 2$ , and

$$f_1(z_1, z_2) = 1 - \frac{1}{z_1^2} - 2i\lambda \left\{ \frac{1}{z_1 - z_2} + \frac{1}{z_1(1 - z_1 z_2^*)} \right\}, \quad (5)$$

$$f_2(z_1, z_2) = 1 - \frac{1}{z_2^2} + 2i\lambda \left\{ \frac{1}{z_2 - z_1} + \frac{1}{z_2(1 - z_2 z_1^*)} \right\}. \quad (6)$$

### III. STATIONARY POSITIONS OF POINT VORTICES

In relation with the experimental observations described in Ref. [3], we will now determine whether there exist stationary locations of the vortex-antivortex pair, both downstream and upstream in the reference frame of the disk. On the complex plane, such stationary positions can only be the complex conjugate points, say,  $z_1^0$  in the upper, and  $z_2^0 = (z_1^0)^*$  in the lower half-plane, respectively. Since the imposed flow is in the positive  $x$ -direction, the velocities of the both vortex points can be zero only in the case where the vortices located at  $z_1^0$  and  $z_2^0$  have the negative and the positive polarity, respectively. This implies  $\Gamma < 0$ , so that the non-dimensional parameter  $\lambda$  defined by the last relation (2) is positive. To ensure that the point vortices located at  $z_1^0$  and  $z_2^0$  are stationary, it is sufficient to require that the complex velocity at  $z_2^0 = (z_1^0)^*$  is zero, i.e.  $f(z_2^0) = f_2(z_1^0, (z_1^0)^*) = 0$ , where the function  $f_2$  is defined by relation (6). Introducing the function  $F(x, y) = yz^*(1 - (z^*)^2)f(z)$ , we obtain the following pair of coupled equations for the coordinates of the stationary point:

$$\text{Im } F(x_1^0, y_1^0) = 0, \quad \text{Re } F(x_1^0, y_1^0) = 0, \quad (7)$$

where

$$\text{Im } F(x, y) = 4xy(y - \lambda)(x^2 - y^2 - 1), \quad (8)$$

$$\text{Re } F(x, y) = (x^2 - y^2)(1 - x^2 + y^2)(y - \lambda) + 4x^2y^2(y - \lambda) - y(1 - x^2 + y^2) + 2\lambda y^2. \quad (9)$$

Consider first Eq. (8). Obviously,  $y_1^0 \neq 0$ . For the root  $y_1^0 = \lambda$ , from Eq. (9) we find  $x_1^0 = \pm\sqrt{1 + \lambda^2}$ , so that  $(x_1^0)^2 + (y_1^0)^2 = 1$ ; this solution corresponds to the vortex points on the disk boundary and should be discarded.

This leaves two families of roots corresponding to  $I^\circ$ :  $1 - (x_1^0)^2 + (y_1^0)^2 = 0$ , and  $\mathcal{D}^\circ$ :  $x_1^0 = 0$ . For family  $I^\circ$  Eq. (9) reduces to  $(y_1^0)^3 - \lambda(y_1^0)^2 + (y_1^0) - \lambda/2 = 0$ . Solution of this equation yields the coordinates  $x_1^0$  and  $y_1^0$ , shown in Fig. 2 (left), of stationary locations of the vortex points. Note the asymptotic behavior,  $x_1^0 \sim \pm\lambda$  and  $y_1^0 \sim \lambda$  as  $\lambda \rightarrow \infty$ .

It can be seen that there exist stationary configurations of the vortex-antivortex pair, both downstream and upstream from the disk; such configurations are symmetric with respect to the  $y$ -axis.

Family  $\mathcal{L}^o$  corresponds to the location of the vortex-antivortex pair on the  $y$ -axis. Setting  $x = 0$ , Eq. (8) yields  $(y_1^0)^4 - \lambda(y_1^0)^3 + 2(y_1^0)^2 - 3\lambda y_1^0 + 1 = 0$ . For  $y_1^0 \geq 1$  (outside the disk) the real solution of this equation is shown in Fig. 2 (right). Note the asymptotic behavior  $y_1^0 \sim \lambda$  as  $\lambda \rightarrow \infty$ .

#### IV. APPARENT STABILITY OF STATIONARY POINTS

The motion of two point vortices whose initial positions are perturbed around the corresponding stationary values, i.e.

$$x_j(0) = x_j^0(\lambda) + (\Delta x_j)_0, \quad y_j(0) = y_j^0(\lambda) + (\Delta y_j)_0, \quad (10)$$

where  $j = 1, 2$ ,  $x_2^0(\lambda) = x_1^0(\lambda)$ , and  $y_2^0(\lambda) = -y_1^0(\lambda)$ , is governed by the system of four Lagrangian equations (4) for  $x_1(t)$ ,  $y_1(t)$ ,  $x_2(t)$ , and  $y_2(t)$ . Numerical solution of Eqs. (4) shows that any perturbation leads in general to sweeping of vortex points by the imposed, uniform at infinity, flow around the disk, so that  $x_j(t) \rightarrow +\infty$  as  $t \rightarrow \infty$  (the only exception being the case of symmetric initial perturbations such that  $(\Delta x_1)_0 = (\Delta x_2)_0$  and  $(\Delta y_1)_0 = (\Delta y_2)_0$ , in which case both vortex points move along closed trajectories around stationary points).

Of particular interest would be an analysis of motion of point vortices during the first  $t_1 = 70$  non-dimensional units of time corresponding to the dimensional duration,  $t_{\text{exp}} = 10$  s of the experiment [3] (see below Sec. V). We will be concerned with the values of  $\lambda$  for which the vortex points, starting their motion near the stationary points  $(x_1^0(\lambda), \pm y_1^0(\lambda))$ , remain in the sufficiently close vicinity of their initial positions for at least  $t_1$  time units. A simple *a priori* estimate for such values of  $\lambda$  can be obtained from Eqs. (4)-(6) as follows. At the stationary positions,  $z_1 = z_1^0(\lambda)$  and  $z_2 = (z_1^0)^*$  we obviously have  $f_{1,2}(z_1^0, (z_1^0)^*) = 0$ . If the vortex point  $z_1(t)$  is located initially in the close vicinity of  $z_1^0$ , so that  $|z_1(0) - z_1^0| \ll |z_1^0|$ , the magnitude of its velocity at  $t = 0$  can be estimated, expanding  $f_1$  around the stationary point, as  $A(\lambda)|z_1 - z_1^0|$ , where

$$A(\lambda) = \left| \frac{\partial f_1(z_1^0, (z_1^0)^*)}{\partial z_1^0} \right|. \quad (11)$$

The function  $A(\lambda)$  is shown in Fig. 3.

If, at  $t = 0$ , the distance between the vortex  $z_1$  and the stationary point  $z_1^0$  is small, the distance traveled by the vortex  $z_1$  during time  $t_1$  can be estimated as  $l \sim A(\lambda)|z_1(0) -$

$z_1^0|t_1$ . Assuming the distance  $l$  to be not larger than few (say, 10) times the initial distance between the vortex and the stationary point, we find that, during the first  $t_1 = 70$  non-dimensional units of time, the vortex point will remain relatively close to its initial position provided  $A(\lambda) \lesssim 0.15$ ; this corresponds to  $\lambda \gtrsim 3$ , see Fig. 3. Consequently, on a time scale corresponding to  $t_1$  non-dimensional units the vortices located sufficiently close to the stationary points  $z_1^0(\lambda)$  and  $(z_1^0(\lambda))^*$  will appear, for  $\lambda \gtrsim 3$ , as apparently stable.

This conclusion is illustrated by the following example. For initial positions defined by the perturbations  $(\Delta x_1)_0 = -0.01$ ,  $(\Delta y_1)_0 = 0.02$ ,  $(\Delta x_2)_0 = -0.03$ , and  $(\Delta y_2)_0 = -0.01$ , the results of numerical calculation of the motion of vortex points are shown in Figs. 4 and 6 (left) for vortices initially located at the rear of the disk, and Figs. 5 and 6 (right) for vortices initially positioned in front of the disk. Our calculations show that, for vortices initially located both at the rear and in front of the disk, the period of time during which the vortex points remain close to their initial locations increases with the non-dimensional circulation  $\lambda$ . For  $\lambda = 3$  the magnitudes of displacement of vortices from their initial locations,  $\Delta r_j = [(x_j - x_j^0)^2 + (y_j - y_j^0)^2]^{1/2}$ , where  $j = 1, 2$ , remain smaller than 0.44 (or less than 15% of the distance from the center of cylinder) for  $t_1 = 70$  time units. This result will be used in Sec. V for explanation of the apparent stability of eddies observed in the experiment [3]. (During the same time interval, a more pronounced displacement such that  $\Delta r_j \sim 1$  occurs already for  $\lambda = 2.8$ .) Note that this conclusion is not a consequence of the specific choice of initial conditions but remains quantitatively valid for any sufficiently small (such that  $|(\Delta x_j)_0| < 0.03$  and  $|(\Delta y_j)_0| < 0.03$ ) initial perturbation.

Similar results were also obtained for the motion of point vortices in the vicinity of family  $\mathcal{P}$  stationary points located at the  $y$ -axis. We found that the point vortices, positioned initially near these stationary points, will remain in their close vicinity during the non-dimensional time  $t_1 = 70$  for considerably larger, compared with those for family  $I^o$ , values of the non-dimensional circulation, i.e. for  $\lambda \gtrsim 7$ ; such values of  $\lambda$  correspond to the stationary points located at  $y_1^0(\lambda) \gtrsim 7$ . Since in the experiment [3] the boundary of the flow domain in the  $y$ -direction was at the distance 6.25 cylinder radii, no apparently stationary flow structures could be observed corresponding to family  $\mathcal{P}$  stationary points. Therefore, for the purpose of this work, the further, more detailed, analysis of the motion of point vortices in the vicinity of family  $\mathcal{P}$  stationary points would be irrelevant.

The numerical results described in this Section can explain, entirely from the classical

fluid dynamics viewpoint without invoking the mechanism of interaction between the normal fluid and superfluid vortices, the apparent stability of the normal eddies observed by Zhang and Van Sciver [3] both at the rear and in front of the cylinder in the thermal counterflow, see Sec. V below.

## V. INTERPRETATION OF EXPERIMENTAL OBSERVATIONS. DISCUSSION AND CONCLUSIONS

In the experiment [3] the velocity field was recorded of a large number of micron-size particles injected in turbulent He II thermal counterflow. In classical viscous fluids, provided a particle is sufficiently small, the viscous drag force exerted on the particle dominates all other forces (such as the inertial and added mass force, Saffman and Magnus lift forces, the Basset memory force, etc.), so that the velocity field of a large, dilute ensemble of solid particles faithfully maps the fluid flow field. In turbulent He II, due to interactions between particles and quantized vortices, particles generally map neither the normal fluid nor superfluid, as was demonstrated by recent experimental [2, 4, 5] and theoretical [6, 7, 9] studies. However, in Zhang and Van Sciver counterflow experiment [3] a tangle of superfluid vortices was rather dilute, with the mean intervortex distance  $\ell \approx 6 \mu\text{m}$  exceeding substantially the particle diameter  $d_p = 1.7 \mu\text{m}$ . This enables us to assume that close encounters between particles and quantized vortices (and, in particular, the events of particle trapping on quantized vortex cores) were relatively rare and, therefore, the particulate flow field recorded in the experiment [3] maps, at least qualitatively, the velocity field of the normal fluid.

Of particular interest are the apparently stationary normal fluid eddies observed by Zhang and Van Sciver both behind and in front of the cylinder. Unlike the familiar Von Kármán vortex street shed by a cylinder, such structures were never observed in the classical viscous flow. In Ref. [3] Zhang and Van Sciver attributed the existence of apparently stationary normal eddies to the mutual friction interaction between quantized vortices and the normal fluid.

In this work we argue that, based on the idealized flow model considered above in Secs. II-IV, the experimental results [3] can be interpreted without invoking the mechanism of interaction between the normal fluid and quantized vortices. It must be emphasized that



the flow analyzed in Secs. II-IV is that of the inviscid fluid, while the normal flow in the experiment [3] is obviously viscous, so that the following arguments and estimates should be regarded as qualitative. However, in the experiment [3] the Reynolds numbers defined by the diameter of the cylinder were at least of the order of  $2 \times 10^4$ , so that the considered inviscid, potential flow can be used as a reasonable approximation to a distribution of the Reynolds averaged velocity of the turbulent normal fluid around the cylinder.

In the experiment described in Ref. [3] the large-scale normal eddies, both downstream and upstream of the cylinder, were observed at a distance about 3 cylinder radii at the angles  $\pm 45^\circ$  and  $\pm 135^\circ$  to the axis through the center of cylinder in the direction of the undisturbed normal flow. For the normal fluid velocity  $v_n \approx 2.2$  cm/s, these circulation patterns appear as stable for the duration of the experiment  $t_{\text{exp}} \approx 10$  s.

Our calculation of motion of point vortices in the imposed potential flow around the disk showed that there exist stationary locations of point vortices, both downstream and upstream of the disk. These locations are unstable: any perturbation of the initial stationary positions of point vortices leads, eventually, to sweeping of point vortices away from their initial locations. The distance between the stationary points and the center of the disk increases with the non-dimensional circulation  $\lambda = -\Gamma/(4\pi Ua)$ . Also increases with  $\lambda$  the period of time during which the slightly perturbed vortex points remain in the close vicinity of the corresponding stationary points. For  $\lambda \gtrsim 3$ , in the case where the magnitudes of initial perturbations of coordinates of stationary positions are smaller than 0.03, we found that the vortices will remain in the close vicinity of the stationary points for at least  $t_1 = 70$  non-dimensional units of time. In the case where the undisturbed fluid velocity,  $U$  and the disk radius,  $a$  are identified, respectively, with the normal fluid velocity,  $v_n \approx 22$  mm/s and the cylinder radius, 3.175 mm in the experiment [3], the corresponding dimensional time is  $t = t_1 a/U \approx 10$  s  $\approx t_{\text{exp}}$ . Therefore, on a time scale corresponding to the duration of experiment [3] the vortices will remain close to the positions of the stationary points and, hence, appear as stable. Moreover, for  $\lambda = 3$  the non-dimensional coordinates of the stationary points,  $x_j^0 \approx \pm 3.005$  and  $y_j^0 \approx \pm 2.834$  correspond to the locations, in the cited experiment, of the observed apparently stable normal eddies at the angles  $\pm 45^\circ$  and  $\pm 135^\circ$  to the axis through the center of the cylinder in the direction of the undisturbed normal flow.

In summary, having considered the motion of the vortex-antivortex pair in the two-

dimensional Euler flow around the disk, we found stationary solutions which enabled us to interpret the existence of apparently stale normal eddies in the experiment [3] without invoking interactions between the normal fluid and quantized vortices. Nevertheless, the mutual friction between quantized vortices and the normal fluid, together with the polarization of the vortex tangle, might be responsible for the emergence of normal eddies in the first place: the polarized cluster of superfluid vortices would rotate the normal fluid (see e.g. Refs. [10, 11]) which, in turn, would drag along the tracer particles in the PIV experiment. (On a related problem, it should be mentioned that the results of Hänninen *et al.* [12] are hinting at the possibility of formation of a classical wake of quantized vortices behind an oscillating sphere. It is not yet known whether a similar phenomenon occurs in the flow past a cylinder, although the experimental results [3] seem to point in this direction.) Assuming that, at least within the domains occupied by the circulation cells observed in the experiment [3], the normal fluid and the superfluid are fully interlocked through the mutual friction, it is easy to estimate that, for the parameters typical of the cited experiment, the value of the non-dimensional circulation,  $\lambda = 3$  corresponds to  $N \approx 2.6 \times 10^4$  quanta of circulation,  $\kappa = 10^{-3} \text{ cm}^2/\text{s}$ . Considering a cluster of  $N$  polarized vortices with a cross-section of radius  $a_{\text{cl}}$ , we find that its (polarized) vortex line density would be  $L' \approx 8.3 \times 10^4 \text{ cm}^{-2}$ , which is a small, 8% polarization of the total (random) vortex line density,  $L_0 \approx 10^6 \text{ cm}^{-2}$  typical of the experiment [3]. Therefore, as envisaged in Refs. [10, 11], even a small polarization of the vortex tangle would be sufficient to generate normal circulation patterns which, if located near the stationary points of the considered Euler flow, can exist as apparently stable for the duration of experiment.

## VI. ACKNOWLEDGMENTS

We are grateful to S. W. Van Sciver, W. F. Vinen, and L. Skrbek for fruitful discussions.

- 
- [1] R. J. Donnelly, A. N. Karpetsis, J. J. Niemela, K. R. Sreenivasan, W. F. Vinen, and C. M. White, *J. Low Temp. Phys.* **126**, 327 (2002); D. Celik and S. W. Van Sciver, *Exp. Therm. Fluid Sci.* **26**, 971 (2002); T. Zhang, D. Celik, and S. W. Van Sciver, *J. Low Temp. Phys.* **134**, 985 (2004); G. P. Bewley, D. P. Lathrop, and K. R. Sreenivasan, *Nature (London)* **441**, 588 (2006).
- [2] T. Zhang and S. W. Van Sciver, *J. Low Temp. Phys.* **138**, 865 (2005).
- [3] T. Zhang and S. W. Van Sciver, *Nat. Phys.* **1**, 36 (2005).
- [4] G. P. Bewley, M. S. Paoletti, K. R. Sreenivasan, and D. P. Lathrop, *Proc. Natl. Acad. Sci. U.S.A.* **105**, 13707 (2008).
- [5] M. S. Paoletti, M. E. Fisher, K. R. Sreenivasan, and D. P. Lathrop, *Phys. Rev. Lett.* **101**, 154501 (2008).
- [6] D. R. Poole, C. F. Barenghi, Y. A. Sergeev, and W. F. Vinen, *Phys. Rev. B* **71**, 064514 (2005).
- [7] Y. A. Sergeev, C. F. Barenghi, and D. Kivotides, *Phys. Rev. B* **74**, 184506 (2006); erratum, *ibid.* **75**, 019904(E) (2007).
- [8] G. K. Batchelor, *An Introduction to Fluid Dynamics* (Cambridge University Press, Cambridge, England, 1967).
- [9] D. Kivotides, C. F. Barenghi, and Y. A. Sergeev, *Phys. Rev. B* **75**, 212502 (2007); *ibid.* **77**, 014527 (2008).
- [10] W. F. Vinen and J. J. Niemela, *J. Low Temp. Phys.* **128**, 167 (2002); erratum, *ibid.* **129**, 213 (2002).
- [11] C. F. Barenghi, S. Hulton, and D. C. Samuels, *Phys. Rev. Lett.* **89**, 275301 (2002).
- [12] R. Hänninen, M. Tsubota, and W. F. Vinen, *Phys. Rev. B* **75**, 064502 (2007).

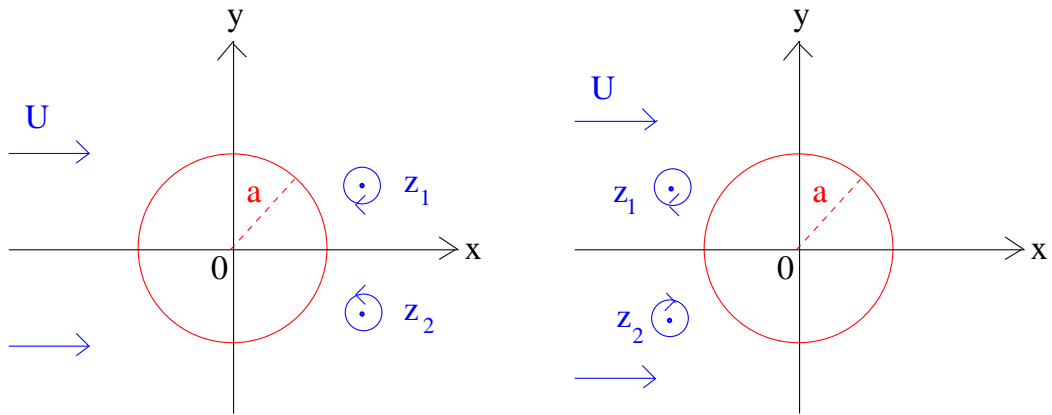


FIG. 1: (Color online). Point vortices in the potential flow around the disk. Left: vortex-antivortex pair downstream (at the rear) of the disk. Right: vortex-antivortex pair upstream (in front) of the disk.

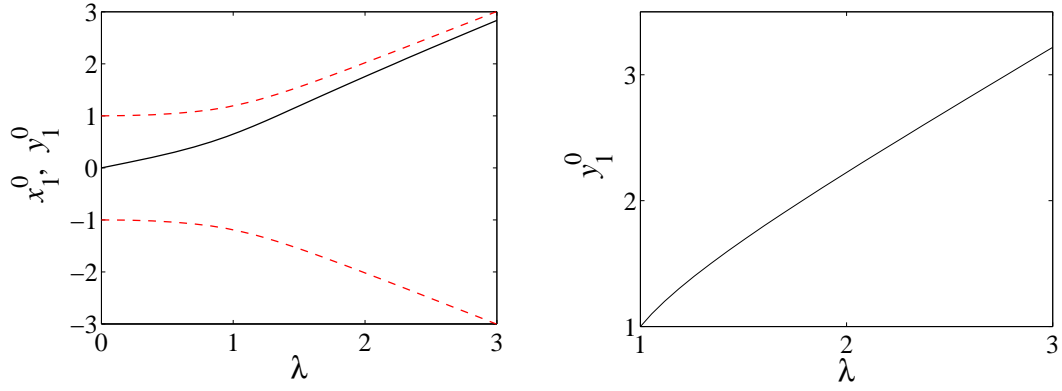


FIG. 2: (Color online). Left: coordinates  $x_1^0$  – dashed (red) lines, and  $y_1^0$  – solid (black) line of the family  $I^0$  stationary points in the upper half-plane as functions of the non-dimensional circulation  $\lambda$ . Right: coordinates of the family  $Z^0$  stationary vortex point in the upper half-plane ( $x_1^0 = 0$ ).

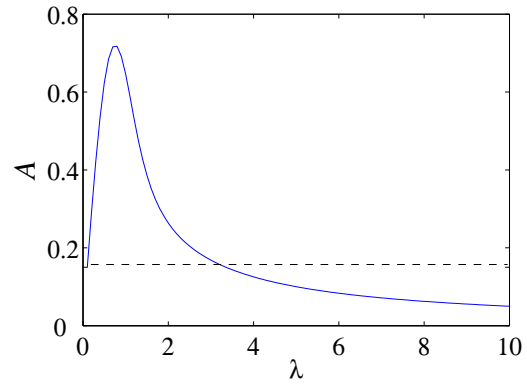


FIG. 3: (Color online). Function  $A(\lambda)$ . The dashed horizontal line corresponds to  $A = 0.15$ .

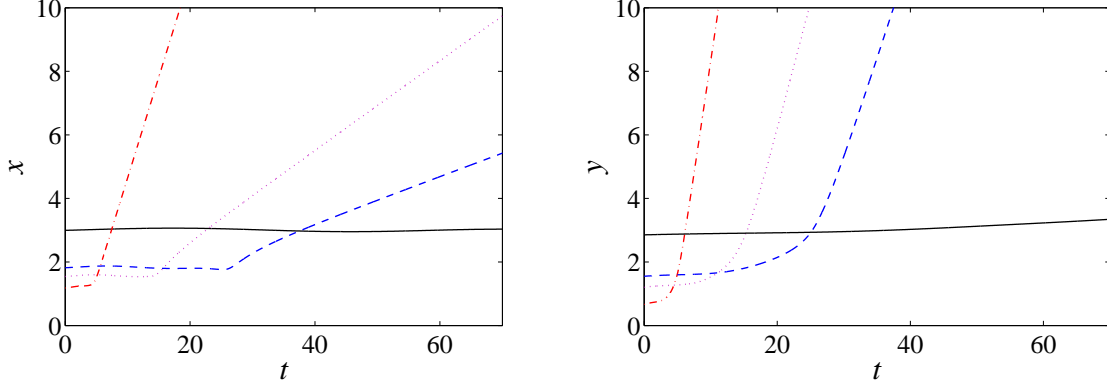


FIG. 4: (Color online). Time-dependent coordinates  $x_1(t)$  (left) and  $y_1(t)$  (right) of the vortex point initially located in the vicinity of the stationary point  $(x_1^0(\lambda), y_1^0(\lambda))$  in the upper half-plane downstream of the disk. Dot-dashed (red) lines:  $\lambda = 1$ ,  $x_1^0 \approx 1.191$ ,  $y_1^0 \approx 0.648$ ; dotted (purple):  $\lambda = 1.5$ ,  $x_1^0 \approx 1.554$ ,  $y_1^0 \approx 1.189$ ; dashed (blue):  $\lambda = 1.8$ ,  $x_1^0 \approx 1.828$ ,  $y_1^0 \approx 1.531$ ; solid (black):  $\lambda = 3$ ,  $x_1^0 \approx 3.005$ ,  $y_1^0 \approx 2.834$ . Initial positions of the vortex-antivortex pair are defined by perturbations  $(\Delta x_1)_0 = -0.01$ ,  $(\Delta y_1)_0 = 0.02$ ,  $(\Delta x_2)_0 = -0.03$ , and  $(\Delta y_2)_0 = -0.01$ .

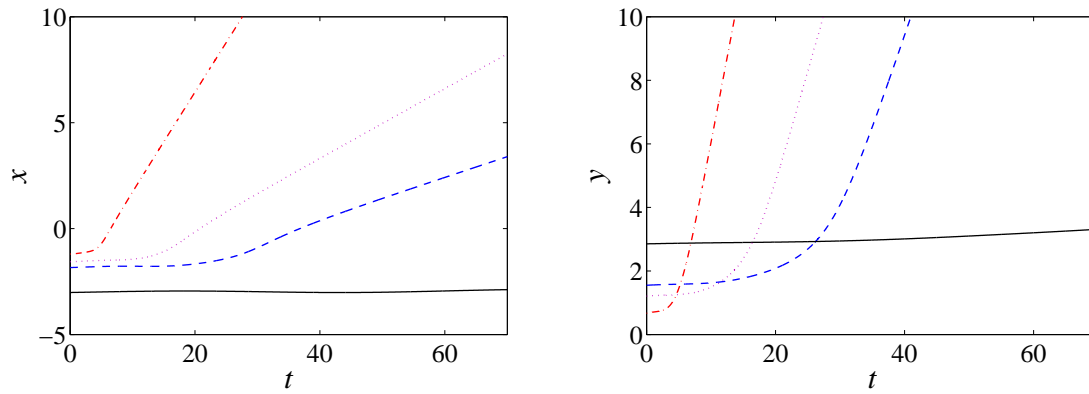


FIG. 5: (Color online). Coordinates of the vortex point initially located in front of the disk. Values of  $\lambda$ ,  $y_1^0(\lambda)$ ,  $|x_1^0(\lambda)|$ ,  $(\Delta x_j)_0$ , and  $(\Delta y_j)_0$  are the same as for Fig. 5.



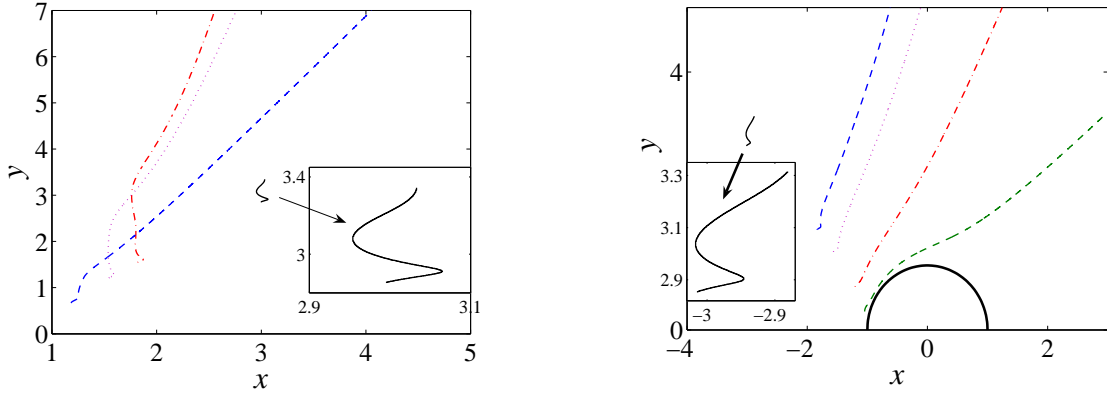


FIG. 6: (Color online). Trajectories of the vortex point. Left: trajectories corresponding to Fig. 4. Right: first four trajectories, from left to right, correspond to Fig. 5; the last trajectory corresponds to  $\lambda = 0.5$  ( $x_1^0(0.5) \approx -1.035$ ,  $y_1^0(0.5) \approx 0.266$ ). Inserts show the trajectories for  $\lambda = 3$  during  $t_1 = 70$  non-dimensional time units.